Cell Adhesion & Migration

ISSN: 1933-6918 (Print) 1933-6926 (Online) Journal homepage: http://www.tandfonline.com/loi/kcam20

Structural abnormalities in the primary somatosensory cortex and a normal behavioral profile in Contactin-5 deficient mice

Kristel T. E. Kleijer, Denise van Nieuwenhuize, Henk A. Spierenburg, Sara Gregorio-Jordan, Martien J. H. Kas & J. Peter H. Burbach

To cite this article: Kristel T. E. Kleijer, Denise van Nieuwenhuize, Henk A. Spierenburg, Sara Gregorio-Jordan, Martien J. H. Kas & J. Peter H. Burbach (2018) Structural abnormalities in the primary somatosensory cortex and a normal behavioral profile in Contactin-5 deficient mice, Cell Adhesion & Migration, 12:1, 5-18, DOI: 10.1080/19336918.2017.1288788

To link to this article: https://doi.org/10.1080/19336918.2017.1288788

Published online: 27 Mar 2017.

CELL ADHESION & MIGRATION
2018, VOL. 12, NO. 1, 5–18
https://doi.org/10.1080/19336918.2017.1288788

Taylor & Francis
Taylor & Francis Group

RESEARCH PAPER

OPEN ACCESS Check for updates

Structural abnormalities in the primary somatosensory cortex and a normal behavioral profile in *Contactin-5* deficient mice

Kristel T. E. Kleijer, Denise van Nieuwenhuize, Henk A. Spierenburg, Sara Gregorio-Jordan, Martien J. H. Kas*, and J. Peter H. Burbach

Department of Translational Neuroscience, Brain Centre Rudolf Magnus, University Medical Centre Utrecht, Utrecht, the Netherlands

ABSTRACT

Contactin-5 (Cntn5) is an immunoglobulin cell adhesion molecule that is exclusively expressed in the central nervous system. In view of its association with neurodevelopmental disorders, particularly autism spectrum disorder (ASD), this study focused on Cntn5-positive areas in the forebrain and aimed to explore the morphological and behavioral phenotypes of the *Cntn5* null mutant (*Cntn5*$^{-/-}$) mouse in relation to these areas and ASD symptomatology. A newly generated antibody enabled us to elaborately describe the spatial expression pattern of Cntn5 in P7 wild type (*Cntn5*$^{+/+}$) mice. The Cntn5 expression pattern included strong expression in the cerebral cortex, hippocampus and mammillary bodies in addition to described previously brain nuclei of the auditory pathway and the dorsal thalamus. Thinning of the primary somatosensory (S1) cortex was found in *Cntn5*$^{-/-}$ mice and ascribed to a misplacement of Cntn5-ablated cells. This phenotype was accompanied by a reduction in the barrel/septa ratio of the S1 barrel field. The structure and morphology of the hippocampus was intact in *Cntn5*$^{-/-}$ mice. A set of behavioral experiments including social, exploratory and repetitive behaviors showed that these were unaffected in *Cntn5*$^{-/-}$ mice. Taken together, these data demonstrate a selective role of Cntn5 in development of the cerebral cortex without overt behavioral phenotypes.

ARTICLE HISTORY
Received 6 September 2016
Revised 3 January 2017
Accepted 26 January 2017

KEYWORDS
autism spectrum disorder; behavior; contactin-5; hippocampus; primary somatosensory cortex

Introduction

Contactin-5 (CNTN5, also referred to as NB2) is a cell-adhesion molecule (CAM), that belongs to the Contactin family of immunoglobulin (Ig)-CAMs. At least 3 members of the Contactin-family (CNTN4, −5, and −6) and 2 members of the Contactin associated protein-like family (CNTNAP2 and −4) have been implicated in ASD genetically through copy number variation analysis.[1-5] CNTN4, −5, and −6 share 40–60% of their amino acid sequence. As far as known, they have characteristic, and distinct expression patterns and appear to serve unique functions in the brain and its development.[6,7]

In addition to ASD, the *CNTN5* gene has been associated with multiple neuropsychiatric traits, including attention-deficient hyperactivity disorder[8] anorexia nervosa[9] and substance abuse.[10] Additionally, genome wide association studies have indicated *CNTN5* as genetic risk factor for Alzheimer disease.[11,12] The biologic basis of these associations, however, remains unknown.

So far, phenotypes caused by deletion of *Cntn5* have been studied in the auditory system on the guidance of the high expression of Cntn5 in auditory nuclei.[13-15] *Cntn5* null mutant mice (*Cntn5*$^{-/-}$) display an unorganized electrical activity pattern in the auditory system. Interestingly, ASD patients carrying *CNTN5* mutations display an increased occurrence of hyperacusis.[4] It remains to be determined if in these patients additional behavioral symptoms arise from other brain systems, and whether *Cntn5*$^{-/-}$ mice have phenotypes other than abnormal auditory functioning. Therefore, we aimed in this study to determine additional sites of *Cntn5* transcript and protein expression in the forebrain and to examine structural and behavioral phenotypes in *Cntn5*$^{-/-}$ mice. The data reveal a selective role of Cntn5 in development of the cortex without ASD-related behavioral deficits.

Methods and materials

Animals

The *Cntn5* knockout mouse line, a generous gift of K. Watanabe and Y. Shimoda, was bred on a C57Bl/6J

CONTACT J. Peter H. Burbach j.p.h.burbach@umcutrecht.nl
Color versions of one or more of the figures in the article can be found online at www.tandfonline.com/kcam.
*Present address: Neurobiology Research Group,Groningen Institute for Evolutionary Life Sciences, University of Groningen, Groningen, the Netherlands.

background in the Brain Center Rudolf Magnus, UMC Utrecht, the Netherlands. In the mutant *Cntn5* was disrupted by an insertion of a Tau-LacZ-Neo cassette in intron 2 of the gene.[13] All mice were group-housed in a Makrolon type III cage (425 × 266 × 185 mm) and received food and water *ad libitum*. For brain analysis, adult and P7 mice were either intraperitoneally injected with pentobarbital (20 mg/kg; Euthanimal, Alfasan), followed by transcardial perfusion or the brains were directly dissected and snap frozen. Behavioral tests were performed with $Cntn5^{-/-}$ and $Cntn5^{+/+}$ male littermates at 3 months of age. For habituation, they were kept in a reversed light-dark cycle 2 weeks in advance of the experiments. Experiments were performed blinded, even as manual scoring. All experimental procedures were in accordance with the Dutch law (Wet op dierproeven, 1996) and European regulations (Guideline 2010/63/EU).

Antibody generation

An antibody against Cntn5 was raised in rabbits against purified protein spanning fibronectin-III domains 1 to 3 ([7], a kind gift of Dr. S. Bouyain). The antiserum was produced by Harlan (Oxford, United Kingdom). This resulted in 2 antisera, from which Cntn5 H4543 was most promising. Consequently, this antiserum was tested and validated.

Immunocytochemistry

HEK293 cells were cultured and transfected with pcDNA3.1-HA-Cntn5 or pcDNA3.1-HA-Cntn6, using polyethylenimine (PEI) as transfection agent. After 48h the cells were fixed with 4% PFA (15 min), washed with PBS and blocked with a blocking buffer (2.5% normal goat serum, 2.5% bovine serum albumin and 0.3% Triton-X). Rabbit anti-Cntn5 H4543 (1:1000) and rat anti-HA (1:500, Sigma-Aldrich) were used (overnight (O/N), 4°C) to detect the expressed proteins. Species-specific secondary antibodies conjugated to Alexa Fluor (1:2000, 2 h, room temperature (RT)) were used and nuclei were stained DAPI (4′,6-diamidino-2-phenylindole; 1:10.000).

Immunoblotting

Brain lysate was prepared from $Cntn5^{+/+}$ and $Cntn5^{-/-}$ mice using a lysis buffer (20 mM Tris-HCl, 150 mM KCl, 1% Triton X-100, 1 mM PMSF and complete protease inhibitor cocktail (Sigma-Aldrich)). Tissue was homogenized by means of sonification and after centrifugation supernatant was collected and β-mercaptoethanol was added at a concentration of 5%. Samples were boiled at 90°C for 5 min. Proteins were separated in an 8% SDS-PAGE gel and transferred onto a nitrocellulose membrane (Amersham Hybond-C Extra). The membranes were blocked at RT for 1 h with 5% milk powder in Tris-buffered saline and tween (TBS-T) and incubated with primary antibody (rabbit anti-Cntn5 H4543, 1:1000) overnight at 4°C. Secondary antibody (goat anti-rabbit peroxidase) was applied at RT for 1 h. Blots were incubated with SuperSignal West Dura Extended Duration Substrate (Pierce) and exposed to an ECL film (Pierce).

Real-time PCR

mRNA was isolated from wild type mice at embryonic stage E12.5, E14.5, E16.4 and E18.5 and postnatal stages P7 and adulthood. One-step qPCR was performed using a Quantifast SYBR Green and RT PCR kit (Qiagen) and a LightCycler (Roche) according to the manufacturer's instructions. The primers were used as follows. GAPDH: Fw CATCAAGAAGGTGGTGAAGC, Rv ACCACCCTGTTGCTGTAG. Cntn5: Fw CAGCAACGTGAGTGGAAGAA, Rv CCTCAAAGGG TGTGAGAGGA.

Immunohistochemistry

Sagittal and coronal sections (40 μm) were obtained from fixed P7 and adult brains. A standard protocol was followed for immunohistochemistry, including a blocking step (1 h; room temperature; 2.5% normal goat serum, 2.5% bovine serum albumin and 0.3% Triton-X in PBS). Sections were incubated with primary antibodies at 4°C O/N. Appropriate secondary antibodies conjugated to Alexa Fluor (1:1000, Invitrogen) were used at RT for 2 h. Primary antibodies were used as follows; rabbit-anti-Cntn5 H4543 (1:500), mouse anti-β-Galactosidase (1:2000, Promega Corp.); rabbit anti-Parvalbumin (1:250, Immunostar), rabbit anti-Synaptoporin (1:1000, Synaptic Systems), mouse anti-Calbindin (1:3000, Swant). Nuclei were visualized with DAPI (1:10.000).

In situ hybridization

Fresh frozen brains from P7 mice were cryosectioned coronally (16 μm) and postfixed with 4% PFA (10 min). *In situ* hybridization was performed according to standard procedures. Digoxigenin (DIG)-labeled RNA probes were used for Cntn5 mRNA or β-galactosidase mRNA. Sections were acetylated and prehybridized, before hybridization was performed with denatured DIG-labeled probe (Cntn5; 800 ng/ml, β-Gal; 1200 ng/ml). Anti-DIG labeled Fab fragments conjugated to alkaline phosphatase (AP) (Boehringer) and AP-labeled antibody, containing levamisole and NBT/BCIP (Roche) were used to detect and visualize the DIG-labeled probes

Nissl staining and structural analysis

Fresh frozen brains from adult *Cntn5*$^{+/+}$ and *Cntn5*$^{-/-}$ animals were cut into coronal sections of 16 μm. The sections were dehydrated in ethanol series, subjected to 0.5% cresyl violet for 10 minutes and dehydrated in ethanol again. Cortical thickness was measured in the primary motor cortex (M1; +0.5 mm to bregma), primary somatosensory cortex (S1; −1.70 mm to bregma) and primary visual cortex (V1; −2.80 mm to bregma). In addition, the upper (I–IV) and lower (V–V1) were measured separately. The surface size of the hippocampus was measured at −1.70 mm to bregma. Measurements were blindly performed by 2 researchers. ImageJ software (1.49 P) was used to measure the areas and IBM SPSS statistics 20 (2011) was used for statistical analysis (independent student's t-test).

Cytochrome C oxidase staining and barrel field analysis

Both cortices were dissected from P7 brains, flattened between silicone-coated glass slides with a 1 mm separator and snap frozen on dry ice. The flattened cortices were cryosectioned at 16 μm thickness. Cytochrome c oxidase staining was performed by incubation with 0.25 mg/ml cytochrome c (Sigma-Aldrich), 40 mg/ml sucrose and 0.5 mg/ml DAB (Sigma-Aldrich) in 1x PBS at 37°C for 6 h. To stop the reaction the slices were washed with PBS.

The barrel field stained with a cytochrome c oxidase reaction in sections of *Cntn5*$^{+/+}$ and *Cntn5*$^{-/-}$ P7 littermates were quantified using ImageJ (1.49 P). Total surface of the posteromedial barrel sub-field (PMBSF) was measured. The surface of the individual barrels was measured, and the sum was subtracted from the total area to calculate the area of the septa. The ratio between surface of the barrels and surface of the septa was calculated and compared between *Cntn5*$^{+/+}$ and *Cntn5*$^{-/-}$ mice. All manual measurements were performed by 2 researchers (K.T.E.K., D.v.N.), who were blind for the genotype. Statistical analysis (independent student's t-test) was performed using IBM SPSS statistics 20 (2011).

Hippocampal formation analysis

Brain sections from *Cntn5*$^{+/+}$ and *Cntn5*$^{-/-}$ mice containing the hippocampus (−1.70 mm to bregma) were stained using antibodies against synaptoporin and calbindin to visualize the mossy fibers and their synapses. Analyses were performed as described in Zuko et al., 2016.[16] In brief, the length, area size and fiber density of the supra- and infrapyramidal bundles (SPB, IPB) were measured. Analyses were performed in 3 sections per hemisphere and at least 28 microscopic images were randomly selected for analyses.

Behavioral tests

Social discrimination

To investigate exploration behavior and memory in a social context, a social discrimination task was performed, as described in Molenhuis *et al.*, 2014.[17] In short, social exploration time was measured upon introduction of a novel intruder mouse. After being exposed to one intruder mouse during the initial exploration period, short-term (5 min) and long-term (24 hours) social memory was tested by introducing both a familiar and a novel mouse in the testing arena. Based on novelty induced exploration behavior, more interest in the novel mouse is expected. The ratio between time spent exploring the novel mouse compared with the familiar mouse was calculated to express social discrimination. A/J male mice (∼P90) were used as social intruders and shifted to the reversed light-dark cycle at least one hour before testing. Due to aggressive behavior, 4 *Cntn5*$^{+/+}$ mice were excluded from the study at time point T0, 2 *Cntn5*$^{-/-}$ mice at T5 and one *Cntn5*$^{-/-}$ mouse at T24. Intervention and exclusion was necessary to prevent harm to the A/J mice and disruption of the interpretation of the social discrimination task.

Object recognition

To examine the exploration behavior and memory for non-social stimuli, an object recognition test was performed, as described in Molenhuis *et al.*, 2014.[17] In brief, object exploration time was measured upon introduction of 2 similar objects. After being exposed to one type of object during the initial exploration period, short-term (1 hour; T1) and long-term (24 hours; T24) memory for objects was tested by introducing both familiar and novel objects in the testing arena. Based on novelty induced exploration behavior, more interest in the novel object is expected. The ratio between time spent exploring the novel object compared with the familiar objects was calculated to express object recognition.

Open field

The open field experiment was performed as described in Molenhuis *et al.*, 2014.[17] In addition to total distance moved, as a measure of novelty-induced activity, the amount of time spent in the inner, middle and outer zone was compared as a parameter for anxiety. Ethovision software (Noldus Information Technology) was used to record and measure the parameters.

Food burying

To confirm the capability to smell, a food burying test was performed. Mice were food deprived for 24 hours before the experiment. One piece of chow was randomly hidden in one of the 4 corners of a Makrolon type IV cage (595 × 380 × 200 mm), just below the upper layer of sawdust. Latency to find the food was measured.

Grooming behavior

To investigate the occurrence of (stress induced) restrictive and repetitive behavior in these mice, *Cntn5*$^{+/+}$, *Cntn5*$^{+/-}$ and *Cntn5*$^{-/-}$ were placed in a clean Makrolon type III cage (425 × 266 × 185 mm). Their behavior was recorded at baseline for 5min. To examine a potential difference in reaction to stress, presented as either a social intruder (age-matched A/J male), a novel object (green piece of Duplo) or nothing, one of these conditions was introduced for 2 minutes. After removal, 5 minutes were recorded for manual scoring of grooming behavior. To increase the efficacy, the mice were subjected to all 3 conditions in a randomized manner, with a period of a week in between. Statistical analysis of the data showed that the order of conditions did not influence the data.

Scoring

All experiments (except for the open field test) were recorded and manually scored using The Observer XT 4.0 software (Noldus Information Technology) afterwards. The experimenter was blinded for the genotypes. To rule out potential bias, a second experimenter scored a random sample of the videos to calculate the intraclass correlation coefficient.

Statistical analyses

For statistical analyses, IBM SPSS statistics 20 (2011) was used to perform separate one-way ANOVA analyses for each behavioral study. Outlier were determined using the outlier labeling rule ($g = 2.2$), which resulted in the removal of 5 data points from different conditions in the grooming experiment. Significance level was set on $p<0.05$. Intra-rater reliability was analyzed using the intraclass correlation coefficient (ICC = (MSB/MSW)/(MSB+(R-1)MSW), in which MSB is mean square between, MSW is mean square within and R is the number of scorers) in SPSS and found to be 0.99 and therefore acceptable.

Results

Expression pattern of Cntn5 protein

To characterize the expression pattern of Cntn5, an antibody against the fibronectin-III domains of Cntn5 (H4543) was generated in rabbits. The specificity was validated in 3 ways: immunocytochemistry, -histochemistry and -blotting (Fig. 1). HEK293 cells transfected with a Cntn5-HA expression plasmid were recognized by the newly generated antibody, whereas native cells and cells transfected with Cntn6-HA expression plasmid were not (Fig. 1A). Both proteins were expressed as demonstrated by an antibody against HA.

For further *in vivo* analyses we first determined the temporal peak of Cntn5 expression Determination of temporal expression of Cntn5 by qPCR indicated that levels of Cntn5 peaked around birth (Fig. 1B). Postnatal day (P) 7 was taken in further studies.

Brain lysates from P7 *Cntn5*$^{+/+}$ and *Cntn5*$^{-/-}$ mice were used for immunoblotting. In the *Cntn5*$^{+/+}$ sample a band just above 130kDa was detected, while this band was absent in the *Cntn5*$^{-/-}$ sample (Fig. 1C). Immunohistochemistry using H4543 showed staining in the inferior colliculus (IC), superior olivary complex (SOC) and the dorsal thalamus of P7 wild type mice. This is in agreement with earlier reports.[13,18] This staining was absent in *Cntn5*$^{-/-}$ mice at age P7 (Fig. 1F–H). These data show that Cntn5 antibody H4543 is suitable to use in a spatial expression analysis.

This antibody was used for elaborate expression analysis of Cntn5, comparing Cntn5 mRNA and protein localization (Tables 1 and 2). The expression analysis showed a limited number of systems with relatively high expression of Cntn5 and a broad expression of Cntn5 at low levels. Cntn5 mRNA and protein were present in the auditory nuclei and dorsal thalamus, in which Cntn5 expression has been described before (Fig. 1, Table 1;[13,18]).

Sites of notably strong and specific expression included the hippocampus, cerebral cortex and mammillary nucleus (MN) (Fig. 2). In the hippocampus Cntn5 mRNA was specifically localized in the granular layer of the dentate gyrus (DG) and the pyramidal layers of the CA1 region. In agreement with this site of expression, Cntn5 protein was found in the molecular layers containing the dendrites of these cells (Fig. 2A–B; Table 1). In the cerebral cortex, Cntn5 mRNA was detected in layer IV, where patches of increased density suggested localization in the barrels of the S1. The protein was found to be located in the lower part of layer IV and layer Va, seemingly localized in the septa between the barrels of S1 (Fig. 2C–F; Table 1). Strong expression of Cntn5 mRNA and protein was also found in the MN.

Notably, Cntn5 protein was localized in the mammillothalamic tract (mt) (Fig. 2G–H; Tables 1 and 2), which connects the MN to the anterior thalamic nuclei.[19]

Anatomical and structural phenotypes in $Cntn5^{-/-}$ mice

The expression of Cntn5 in the cerebral cortex and hippocampus lead us to examine the organization of these regions in $Cntn5^{-/-}$ animals in comparison to wild-type littermates.

Structural abnormalities in S1 of $Cntn5^{-/-}$ mice

Morphometry of the cerebral cortex of adult male littermates revealed a reduction in the thickness of the primary somatosensory cortex (S1) in the $Cntn5^{-/-}$ animals (Fig. 3A–C) This thinning was not observed in the primary motor (M1) and primary visual cortex (V1) (Fig. 3C). The significant reduction in the S1 was particularly due to a significant decrease in thickness of layers IV-VI (Fig. 3C).

In S1, *Cntn5* mRNA showed patches of increased density, suggesting localization to the barrels of layer IV of the S1 (Fig. 2F), whereas the Cntn5 protein seemed to be localized in the septa between the barrels (Fig. 2D,E). The septal localization of Cntn5 suggested the possibility of synaptic expression originating from Cntn5-positive afferent neurons in the posterior nuclear group of the thalamus (Po) (Table 1). To compare the localization of cortical Cntn5-expressing cells between null mutants and wild-type mice, we performed *in situ* hybridization in adult $Cntn5^{+/+}$ and $Cntn5^{-/-}$ mice. Advantage was taken of the Tau-LacZ-Neo cassette incorporated in the *Cntn5-* gene in the $Cntn5^{-/-}$ animals, to localize Cntn5-expressing cells by presence of β-galactosidase mRNA.[18] An apparent difference was observed. In $Cntn5^{+/+}$ animals, Cntn5 mRNA was detected in layer IV of the S1

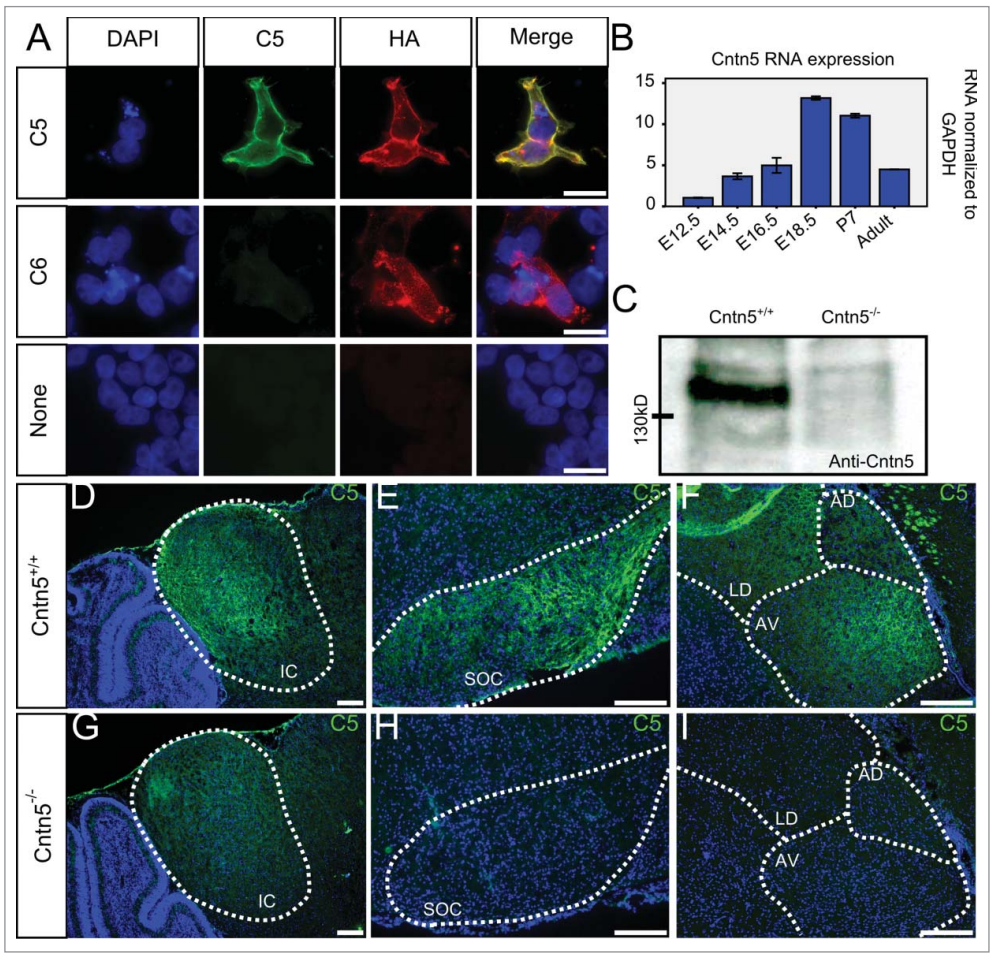

Figure 1. Rabbit-α-Cntn5 specifically binds Cntn5 in wild type brain tissue. Rabbit-α-Cntn5 binds specifically to Cntn5 transfected in HEK293 cells, while it does not bind Cntn6 transfected in HEK293 cells. Both transfections were confirmed by staining of the HA-tag. HEK293 that did not receive any transfection were not recognized by either antibody (A). Real-time PCR analysis different developmental stages demonstrates high levels of Cntn5 RNA at E18.5 and P7 (B). On Western blot, the antibody only shows Cntn5 protein in brain tissue from $Cntn5^{+/+}$ animals, but not in tissue from $Cntn5^{-/-}$ mice (C). Known areas of expression are stained by rabbit-α-Cntn5 in $Cntn5^{+/+}$, but not in $Cntn5^{-/-}$ mice (D-I), except from mild background staining in the IC (G). Scalebars; 20μm (A), 200 μm (D-I), abbreviations IC; inferior colliculus, SOC; superior olivary complex, LD; laterodorsal thalamic nucleus, AD; anterodorsal thalamic nucleus, AV; anteroventral thalamic nucleus.

Table 1. Cntn5 mRNA and protein localization in the mouse brain.

Area	Cntn5 mRNA	Cntn5 Protein	Area	Cntn5 mRNA	Cntn5 Protein
Telencephalon			**Amygdala**	+	+
Accessory olfactory bulb			**Caudate putamen**	+	+
- Mitral layer	+	+	**Accumbens nucleus**	+	
- Granular layer	+		*Diencephalon*		
Olfactory bulb			**Thalamus**		
- Mitral layer	+	+	- Lateral dorsal nucleus	++	++
- Glomerular layer	+	+	- Lateral posterior nucleus	+	+
- Granular layer	+	+	- Lateral habenula	+	
Anterior olfactory nucleus	+		- Lateral geniculate complex	+	+
Piriform cortex	++	++	- Medial geniculate complex	+	+
Neocortex			- Centrolateral nucleus		+
- Layer II/III			- Anteroventral nucleus	+	+
- Layer IV	+	+	- Mediodorsal nucleus	+	+
- Layer V	+/−	+	- Anteromedial nucleus		+
- Layer VI			- Anterodorsal nucleus	+	
Entorhinal cortex	+	+	- Posterior nuclear group	+	+
Hippocampal formation			- Other	+/−	+/−
- Parasubiculum	+	+	**Hypothalamus**		
- Postsubiculum	+	+	- Ventromedial nucleus	+	
- Presubiculum	+	+	- Zona incerta	+	+
- Subiculum	+	+	- Premammillary nucleus	+	
- CA1			- Mammillary body		
-Lacunosum moleculare		+	-Medial mammillary nucleus	++	++
-Pyramidal layer	+		-Lateral mammillary nucleus	++	++
- CA2			-Supramammillary nucleus	++	+
-Lacunosum moleculare		+/−	-Diffuse	+/−	+/−
-Pyramidal layer			*Midbrain*		
- CA3			**Inferior colliculus**	++	++
-Lacunosum moleculare			*Pons*		
-Pyramidal layer			**SOC**	++	++
-Stratum lucidum		+	**Ventral nucleus of lateral lemniscus**	+	
- Dentate gyrus			*Cerebellum*		
-Molecular layer		+	**Purkinje cell layer**	+	+
-Granular layer	+				

(Fig. 3D, D'), whereas in *Cntn5*$^{-/-}$ mice β-galactosidase mRNA was detected in layer V of the S1 (Fig. 3E, E'). Since β-galactosidase was expressed instead of Cntn5 in *Cntn5*$^{-/-}$ mice, it shows that Cntn5-ablated cells were misplaced. The ectopic *Cntn5*$^{-/-}$ cells found in the lower layers of the S1, may suggest that in the absence of Cntn5 neuronal migration is affected.

Table 2. Cntn5 protein localization in fiber tracts in the mouse brain.

Fiber tract	Cntn5
Internal capsule	+
External capsule	+
Anterior commissure	+
Intrabulbar anterior commissure	+
Ventral hippocampal commissure	+
Dorsal hippocampal commissure	+
Thalamocortical tract	++
Principal mammillary tract	+
Mamillothalamic tract	++
Medial lemniscus	+
Lateral lemniscus	
External medullary lamina of thalamus	
Cingulum	
Superior thalamic radiation	
Fasciculus retroflexus	+
Corpus callosum	+
Fimbria	++
Fornix	+
Cerebral peduncle	+

Analysis of expression of Cntn5 in cortical cell-types using the cell taxonomy tool offered by the Allen institute (http://casestudies.brain-map.org;[20]), showed that Cntn5 was expressed in pyramidal neurons, and in neuron-derived neurotrophic factor-positive and parvalbumin-expressing interneurons. To determine whether both pyramidal neurons and interneurons were affected by Cntn5-deletion, co-staining for β-galactosidase and parvalbumin was performed on Cntn5$^{-/-}$ brains. Both parvalbumin-positive interneurons (Fig. 3F) and parvalbumin-negative cells (Fig. 3G) were found among the Cntn5-ablated cells in layer V.

Changes in the barrel field of Cntn5$^{-/-}$ *mice*

Cntn5 is expressed in the rostral and medial parts of the thalamic Po (Table 1) which innervate the septa of the PMBSF.[19] The expression of *Cntn5* in the thalamocortical system, in particular the expression in the Po, as well as the cortical layer-specific expression lead us to examine the organization of the PMBSF in *Cntn5*$^{-/-}$ mice. Cytochrome C oxidase staining in P7 littermates showed

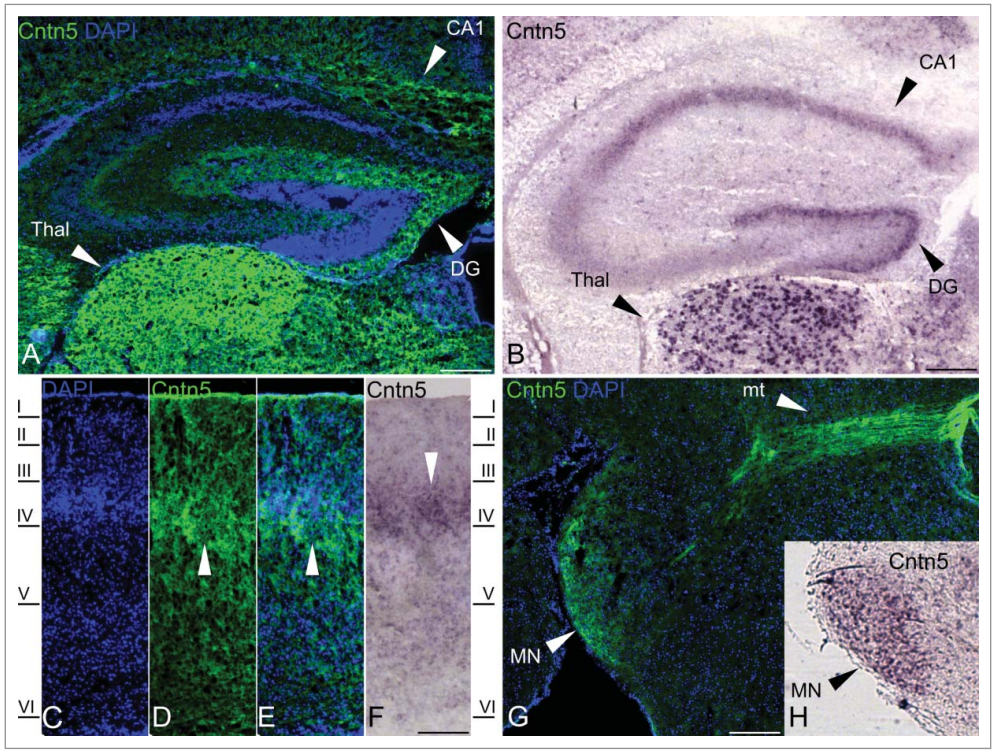

Figure 2. Additional areas of characteristic Cntn5 expression. Besides well described areas of expression, such as nuclei in the auditory pathway and the dorsal thalamus, A,B) Cntn5 protein and mRNA is present in the DG and CA1. In the cerebral cortex, C-F) Cntn5 expression is restricted to layer IV-V, where the protein seems to most prominently localize in the septa between the barrels and the mRNA localizes to the barrels. G,H). Clear and strong expression of Cntn5 is observed in the MN and mt. Scalebars; 200μm. Thal; thalamus, CA1; field CA1 of the hippocampus, DG; dentate gyrus, MN; mammilary nucleus, mt; mammilothalamic tract.

no significant difference in the pattern and total surface of the PMBSF (data not shown). However, the ratio between barrel surface and septa was significantly larger in the *Cntn5*$^{-/-}$ mice (Fig. 3H–J; n = 4, 4, p = 0.001), indicating that the organization of the PMBSF was affected by Cntn5 deficiency.

Absence of abnormalities in hippocampal formation of Cntn5$^{-/-}$*mice*

Next, we analyzed the hippocampus in view of Cntn5 expression in CA1, CA2 and the DG (Table 1). Nissle staining in the hippocampus of adult male littermates (Fig. 4A, E) allowed measurements of the surface area of the hippocampal formation. No significant difference was found in hippocampal size (Fig. 4I). It is known that several CAMs affect the integrity and fasciculation of the IPB and SPB, including close homolog of L1 (Chl1), a relative of contactins.[21,22] General parameters of the IPB and SPB were measured using established markers. Synaptoporin (Spo) is robustly expressed as a presynaptic marker of the IPB and SPB. Calbindin (Calb) was used as second marker and visualizes cell bodies in the DG granule cells and axons. No difference in length (Fig. 4J) and area (Fig. 4K) of the IPB, SPB, or in the ratio of length and area between the bundles (data not shown) was found. Only few mossy fibers of the IPB crossed the stratum pyramidale (SP) before the IPB is terminated. Quantification of the fibers crossing the SP revealed no differences between *Cntn5*$^{+/+}$ and *Cntn5*$^{-/-}$ animals (Fig. 4L). The data demonstrate that these aspects of the hippocampal formation are not affected in *Cntn5* mutant mice.

Behavioral analyses of Cntn5$^{-/-}$ *mice*

To gain insight into the function of Cntn5 and a potential effect of a mutated variant on behavior, a set of behavioral paradigms was selected that provided relevant read-outs with regard to both the sites of expression as the association with neurodevelopmental disorders. These paradigms included social exploration and interaction, object and environmental exploration, anxiety, odor detection and memory.

Social exploration and recognition

To test social behavior, a social exploration and recognition task was performed. To examine social exploration behavior, an age-matched A/J male mouse was introduced to *Cntn5*$^{+/+}$ and *Cntn5*$^{-/-}$ mice for 2 minutes. The time for exploration of the novel mouse did not significantly differ between *Cntn5*$^{+/+}$ (n = 12) and

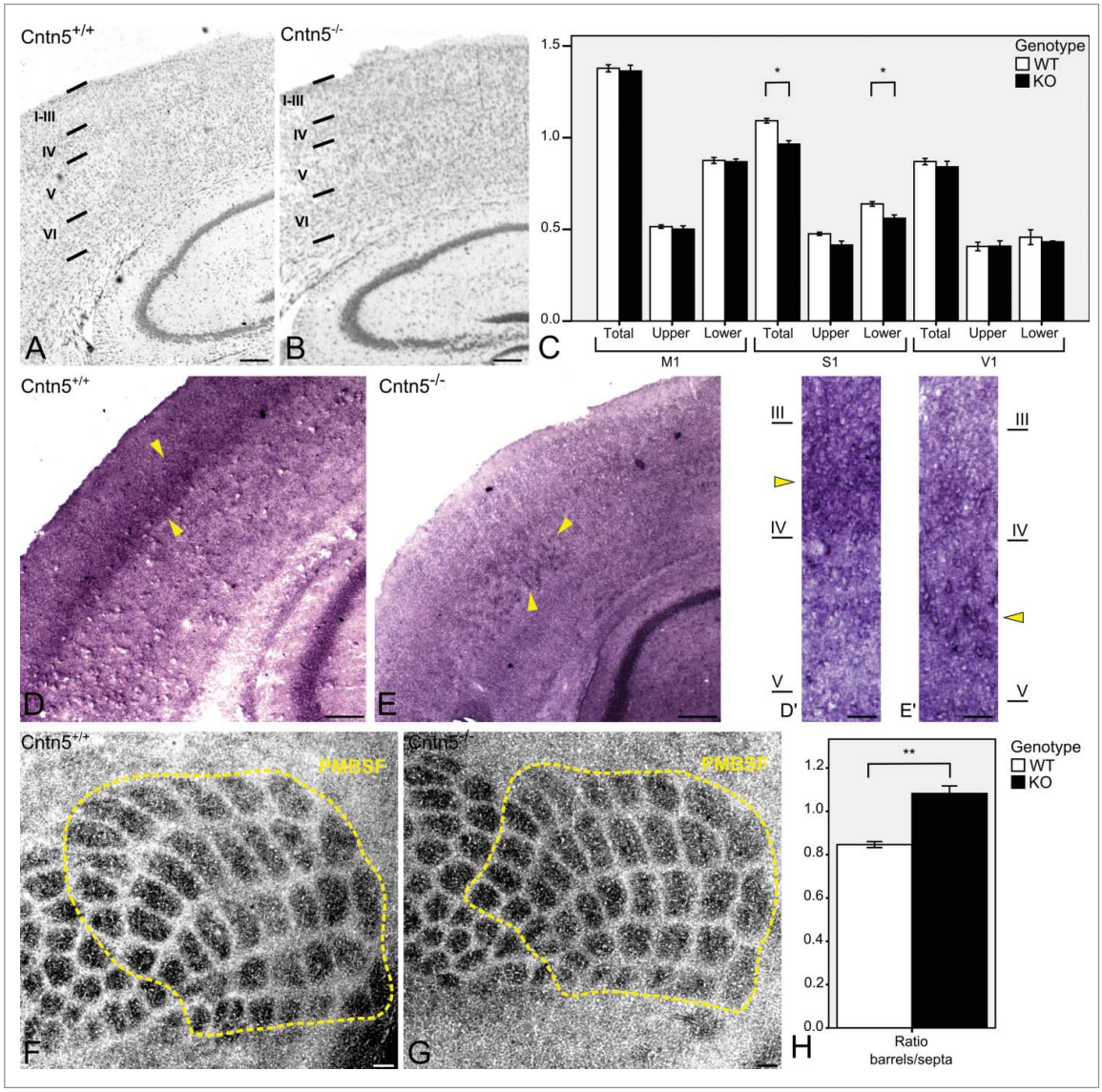

Figure 3. Structural abnormalities in the S1 in Cntn5$^{-/-}$ mice. Cortical thickness is reduced in Cntn5$^{-/-}$ mice (B) compared with control littermates (A) in S1 (C; n = 5, 4, total p = 0.019, upper p = 0.289, lower p = 0.012), but not in M1 (C; n = 5, 4, total p = 0.995, upper p = 0.755, lower p = 0.819) and V1 (C; n = 4, 4, total p = 0.440, upper p = 0.967, lower p = 0.410). Cntn5 mRNA is located in layer IV of S1 in adult wild type mice (D, D′). bGal mRNA is found in layer V of S1 in adult Cntn5$^{-/-}$ mice (E, E′). PMBSF was measured in P7 Cntn5$^{+/+}$ mice (F) and compared with the PMBSF in P7 Cntn5$^{-/-}$ mice (G) a greater ratio between barrel and septa surface was detected (H; n = 4, 4, p = 0.001). Scalebars A-B, D-E, F-G; 200 μm, D′-E′; 50 μm. Data is represented as mean ± SEM. M1; primary motor cortex, S1; primary somatosensory cortex, V1; primary visual cortex, bGal; β-galactosidase, PMBSF; posteromedial barrel sub-field.

Cntn5$^{-/-}$ (n = 12) mice (Fig. 5A), suggesting similar interest in novel social encounters. With a comparable baseline level of exploration time the genotypes could be compared on their short-term (5 minutes) and long-term (24 hours) memory for social interaction. Both genotypes showed preference for exploring the novel mouse after 5 minutes (WT n = 12, KO n = 10) (Fig. 5B), with no significant difference in performance. After 24 hours the mice spent slightly more time exploring the novel mouse. This did not differ between genotypes (WT n = 12, KO n = 9) (Fig. 5B).

Object exploration and recognition

To investigate whether novelty seeking behavior was affected, one of 3 types of inanimate objects (a glass, a plastic or a metal bottle) was placed in the cage of *Cntn5*$^{+/+}$ and *Cntn5*$^{-/-}$ mice. Exploration time did not significantly differ between *Cntn5*$^{+/+}$ (n = 16) and *Cntn5*$^{-/-}$ (n = 12) mice (Fig. 5C). To test whether Cntn5 deficiency influences learning and recognition memory processes, a novel object recognition test was performed. Both *Cntn5*$^{+/+}$ (n = 15) and *Cntn5*$^{-/-}$ (n = 12) animals were capable of recognizing the familiar

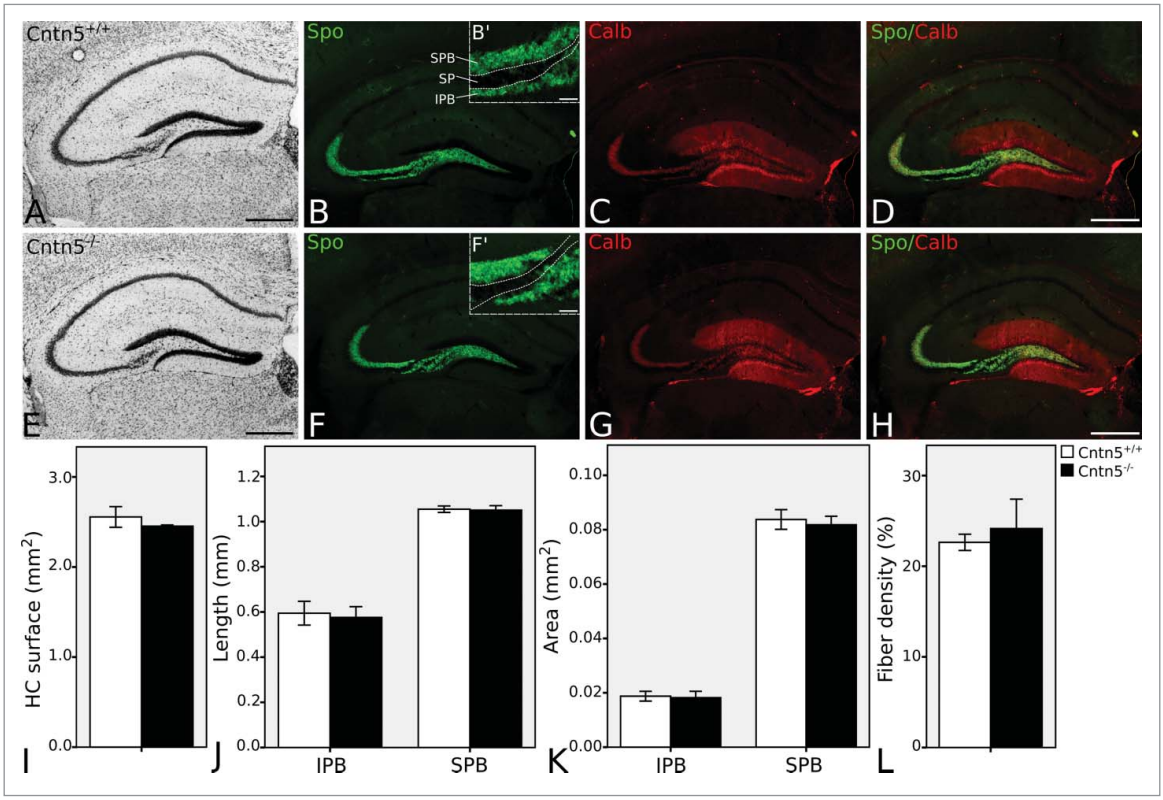

Figure 4. Normal mossy fiber distribution in the hippocampal formation of Cntn5$^{-/-}$ mice. Total surface area measurements of the hippocampal formation in Nissle staining (A,E) revealed no abnormalities (I; n = 3, 5, p = 0.541). Visualized with staining of Spo and Calb, the IPB and SPB of Cntn5$^{+/+}$ (B-D) and Cntn5$^{-/-}$ (F-H) mice were measured. Length (J; n = 3, 5, IPB p = 0.800, SPB p = 0.880) and area (K; n = 3, 5, IPB p = 0.864, SPB p = 0.695) of the IPB and SPB were not different, even as the ratio between the 2 (data not shown). Fibers crossing the SP were quantified in Cntn5$^{+/+}$ and Cntn5$^{-/-}$ mice. No significant difference was found (L; n = 3, 5, p = 0.698). Scalebars A-H; 500μm, B', E'; 50μm. Data is represented as mean ± SEM. Spo; synaptoporin, Calb; calbindin, HC; hippocampus, SPB; suprapyramidal bundle, SP; stratum pyramidale, IPB; infrapyrimidal bundle.

object after a short period (1 hour) and a prolonged period (24 hours). They did not perform significantly different (Fig. 5D).

Environmental exploration, anxiety and odor detection

To test environmental exploration levels, anxiety and odor detection in the mice, and to simultaneously confirm the general health parameters of locomotion and smell, 2 tests were selected. As a measure of environmental exploration, movement patterns and distance traveled in a round open field arena were analyzed. No difference between the genotypes (WT n = 16, KO n = 12) was detected (Fig. 5E). *Cntn5*$^{+/+}$ and *Cntn5*$^{-/-}$ mice spent most time in the outer and least time in the inner zone, without significant difference between the genotypes. This result suggested that both Cntn5 genotypes had similar anxiety levels (Fig. 5F). Although *Cntn5*$^{-/-}$ (KO; n = 12) took slightly longer to find the food buried in a corner, their performance did not significantly differ with *Cntn5*$^{+/+}$ (WT; n = 15) mice (p = 0.254).

Grooming behavior

As a measure for repetitive and restrictive behavior, we analyzed novelty-induced grooming behavior in the *Cntn5*$^{-/-}$ mice and their *Cntn5*$^{+/-}$ and *Cntn5*$^{+/+}$ littermates. During the first 5 minutes in a clean cage (baseline), *Cntn5*$^{+/+}$ (n = 10), *Cntn5*$^{+/-}$ (n = 13) and *Cntn5*$^{-/-}$ (n = 17) spent similar time grooming (Fig. 5G). To measure grooming behavior as a reaction to different stressful situations, a novel social intruder, an object or nothing was introduced for 2 minutes. The genotypes responded similarly to any of the conditions, though the time spent on grooming tended to increase after intrusion, in all 3 conditions compared with baseline. However, significance levels were not reached (Fig. 5H). No effect on frequency and therefore bout duration was detected (data not shown).

Discussion

In genetic studies, *CNTN5* has been associated with neurodevelopmental disorders, in particular with ASD. However, understanding of functions of CNTN5 in the development of the brain is to this date very limited. To this purpose, we

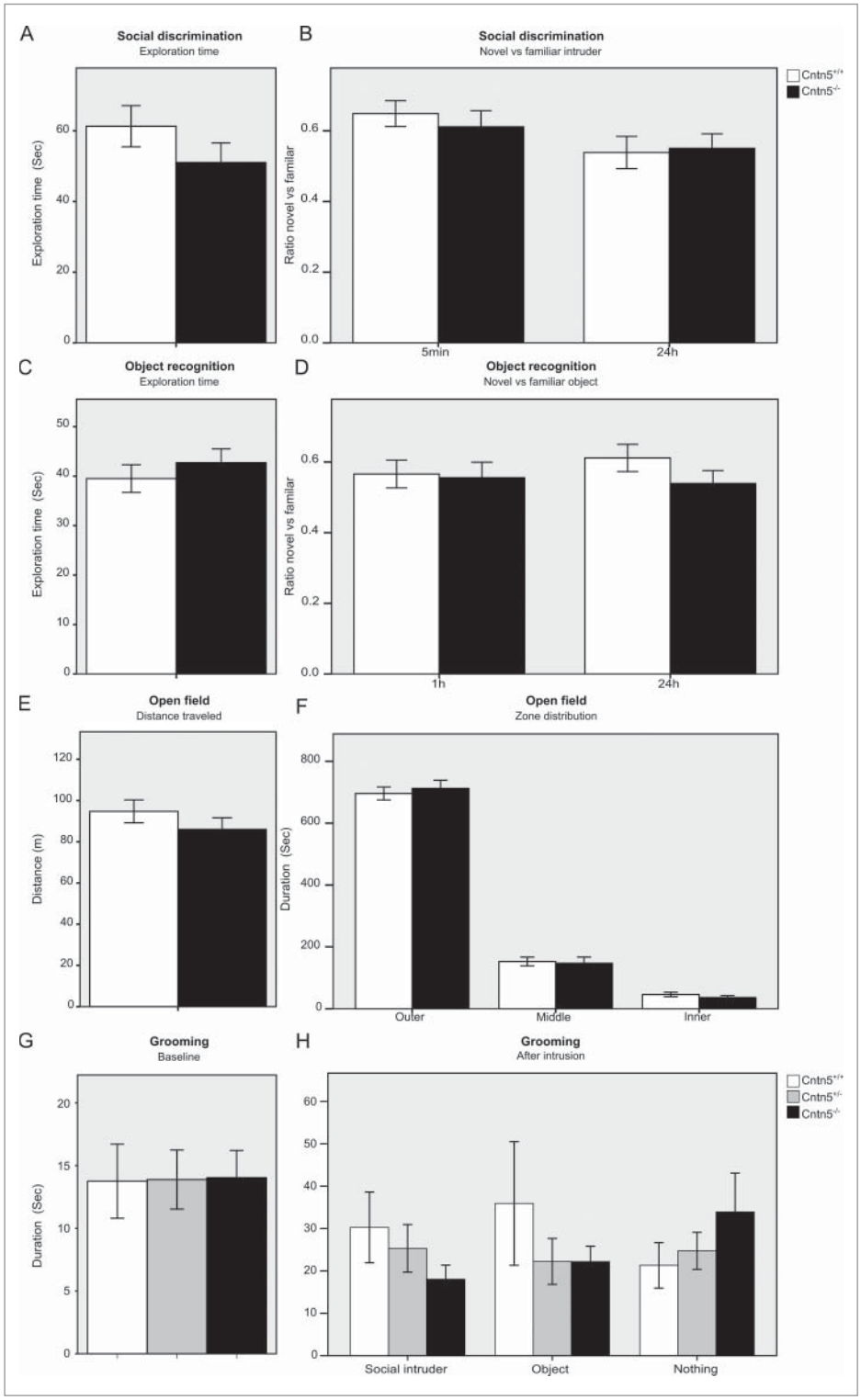

Figure 5. Cntn5$^{-/-}$ show no abnormalities in this set of behavioral experiments. No significant difference was detected in the time spent exploring a newly introduced animal (A; n = 12, 12, p = 0.214), nor in the recognition of the familiar mouse after 5 min (B; n = 12, 10, p = 0.524) and 24h (B; n = 12, 9, p = 0.853). Both genotypes spent comparable amount of time exploring a newly introduced object (C; n = 16, 12, p = 0.461) and showed to recognize the familiar object after 1h and 24h (D; n = 15, 12, 1h p = 0.812, 24h p = 0.172). In an open field both genotypes traveled the same distance (E; n = 16, 12, p = 0.292) with the same velocity (data not shown). No difference was seen in anxiety level based upon zone distribution in the open field (F; n = 16, 12, outer p = 0.632, middle p = 0.817, inner p = 0.351). At baseline no significant difference was found between Cntn5$^{+/+}$, Cntn5$^{+/-}$ and Cntn5$^{-/-}$ in grooming behavior (G; n = 10, 13, 17, p = 0.997). Similarly, after stressful intrusion, either by an object, novel social intruder or nothing no significant difference in grooming behavior was observed between the genotypes (H; n = 10, 13, 17, object p = 0.395, intruder p = 0.281, nothing p = 0.472). Data is represented as mean ± SEM.

have investigated the consequences of Cntn5 deficiency in mice on brain morphology and behavior related to ASD in mice with focus on the forebrain.

We first determined the expression pattern of Cntn5 in the mouse brain. Our data show that Cntn5 mRNA is present at high level around birth and remained high in the first postnatal week (Fig. 1B), confirming previous findings. This temporal course coincides with the highly dynamic phase of maturation of brain circuits involving neuronal wiring, synaptogenesis and pruning.[13,18,23] The detailed spatial expression pattern presented here (Tables 1 and 2) demonstrate that high Cntn5 expression is restricted and confined to specific brain systems. Similar restricted expression exists for Cntn4 and Cntn6, the most related contactins.[16,24] Notably, neurons expressing these genes are sometimes in in close proximity to Cntn5 expression, for instance in the cortex and thalamus, but are barely overlapping. This suggests non-redundancy in brain functioning.

In addition to the function of Cntn5 in auditory nuclei of the brain,[13] the current study indicates a multifold role of Cntn5 in the development of the cortex, in particular the S1 region. The expression of Cntn5 in subsets of pyramidal neurons and in thalamic nuclei innervating the S1 constitutes a complex organization. Clear phenotypes in absence of Cntn5 were detected in the S1. Cortical thickness was significantly reduced, Cntn5-ablated cells were misplaced and the PMBSF was affected (Fig. 3). How and whether these phenotypes are related and stem from the same cause remains undetermined due to the complex integration of Cntn5-expressing systems in the cortex.

One hypothesis may involve immature synaptic connections between cortically expressed Cntn5 and Cntn5-positive presynaptic afferents from the thalamus. The PMBSF represents the 5 major rows of mysticial vibrissae and is innervated by projections from the thalamus. Previous studies have shown that Cntn5-deficiency leads to a disorganized activity pattern in the IC. Narrow frequency selective bands were developed in the IC in an activity-dependent manner.[13] Further studies revealed that disruption of *Cntn5* leads to immature synaptic-terminals in the auditory regions of the brain. As a consequence of the failure to mature, the cells went into programmed cell death, leading to significantly increased apoptosis and a decrease in cell number.[14] In Cntn6-deficient mice an abnormal distribution of neurons in the cerebral cortex was described and interpreted to be due to an increase in apoptosis.[16] A failure to mature the presynaptic-terminals coming from Cntn5-positive thalamic nuclei, such as the Po, and therewith a failure to connect to cortical neurons may explain the reduction in cortical thickness and increased barrel/septa ratio of the PMBSF. The migration deficit observed in the S1 of Cntn5-deficient mice would in this hypothesis stand on its own.

Alternatively, the PMBSF may be affected by the evident misplacement of Cntn5-ablated cells in the S1 (Fig. 3D–E). The paralemniscal pathway, in which neurons from rostral and medial Po innervate the septal columns of the PMBSF, is dependent on the state of the corresponding cortex.[25] As a consequence of the misplacement of the Cntn5-ablated neurons, innervation, and therewith the proportions, of the septal columns may be influenced.

Interestingly, cortical thinning was only detected in the S1, while the Cntn5-positive M1 and V1 were unaffected in absence of Cntn5. This has been observed with regard to other CAMs as well. In Cntn6-deficient mice disturbed neuronal distribution in V1 was described.[16] Though the current data are not sufficient to explain the restricted effect on the S1, we hypothesize that projections from the Cntn5-deficient thalamic nuclei may be responsible. The V1 receives input from the thalamic geniculate nuclei. Expression of Cntn5 in these nuclei was less apparent. Projections from the Po and VL both reach the S1 and M1, however, it may be hypothesized that only the cells projecting to the S1 are Cntn5 positive.[19] This may explain the restricted effect on the S1 in Cntn5-deficient mice.

Several IgCAMs have shown to be involved in the development of the dentate gyrus (DG) of the hippocampus. Analysis of the SPB and IPB have shown that deletion of ChL1,[21,22] NCAM[26] and Cntn6,[16] for instance, affect the distribution of the mossy fibers of the hippocampus, likely due to impairing fasciculation. Cntn5 was shown to be expressed in the CA1, CA2 and DG (Fig. 2A–B, Table 1). The structural analysis of the hippocampus did not indicate any abnormalities in the *Cntn5*$^{-/-}$ mice (Fig. 4), showing that Cntn5 does not have an essential function in this axonal bundle.

With regard to the association with ASD and the regions with strong expression, an effect of Cntn5-deficieny on behavior needed to be determined. To date there are no studies that describe the behavior of Cntn5-deficient mice.[7] We selected a set of relevant behavioral paradigms to model quantifiable behavioral phenotypes, such as a social exploration and grooming behavior, related to ASD domains, respectively social interaction and repetitive behavior. Furthermore, we focused on behavioral paradigms which were prone to express abnormalities on the basis of the observed expression pattern of Cntn5 (Table 1). Impaired social exploration and interaction are included in the diagnostic criteria for ASD, but no indication for an abnormality in Cntn5-deficient mice was found (Fig. 5A). Other novelty seeking behavior, such as object and environmental exploration levels have been reported to be reduced in

individuals with ASD,[27,28] and in mouse models of ASD.[29] No such impairment was found in *Cntn5*-mutated mice (Fig. 5C, E). One of the key characteristics of ASD is repetitive and restrictive behavior, which may be represented by grooming behavior in rodents.[30] Cntn5-deficient animals did not show aberrant grooming behavior (Fig. 5G–H). Other behavioral parameters, were selected based upon strong sites of expression or for the relation to ASD. For example, the social and object recognition was chosen because of Cntn5 expression in the hippocampal formation and perirhinal cortex (Fig. 2A, B, Table 1,[31]), and anxiety and odor detection were chosen for their relation to ASD.[32] However, none of these were indicated to be altered by Cntn5-deficiency (Fig. 5). No aberrations were detected with the current selection of behavioral tests.

The normal behavior of Cntn5-deficient animals may suggest that a genetic compensatory mechanism might be at play, reducing the effect of the mutation. Secondly, by selecting a set of behavioral experiments, other behavioral paradigms were excluded. Deficiency of ASD-risk gene Cntn4 in mice was found to cause no aberrations in autism-like behavior, but did affect sensory behavior and cognitive performance.[33] Elaboration of the set of behavioral experiments and including a set of experiments during the development, may bring a subtle behavioral phenotype to view. These data suggests that disruption of Cntn5 has no or limited influence on social, explorative and repetitive behavior in our mouse model.

The current study provides an expression map of Cntn5 in P7 mice. The morphological phenotype found in the S1 and PMBSF, may be caused by synaptic or migratory defects. Though the very specific expression pattern of Cntn5 suggests functional non-redundancy and deletion results in a clear structural phenotype in the S1, no consequential behavioral phenotype was detected.

Abbreviations

AP	Alkaline phosphatase
ASD	Autism spectrum disorder
BCIP	5-Bromo-4-chloro-3-indolyl phosphate
CA1,2,3	Cornu ammonis 1,2,3
Calb	Calbindin
CAM	Cell-adhesion molecule
Chl1	Close homolog of L1
Cntn	Contactin
CNTNAP	Contactin associated protein-like family
°C	Degrees Celcius
DAPI	4′,6-diamidino-2-phenylindole
DG	Dentate gyrus
DIG	Digoxigenin
DNA	DNA
E18.5	Embronic day 18.5
ECL	Enhanced chemiluminescence
h	Hour
HCl	Hydrochloric acid
HEK293	Human embryonic kidney cells
IC	Inferior colliculus
ICC	Intraclass correlation coefficient
IgCAM	Immunoglobulin cell adhesion molecule
IPB	Infrapyramidal bundle
kDa	Kilodalton
kg	Kilogram
KO	Knockout
M1	Primary motor cortex
MN	Mammillary nucleus
(m)RNA	(Messenger) Ribonucleis acid
MSB	Mean square between
MSW	Mean square within
mg	Milligram
ml	Milliliter
mm	Millimeter
mM	Millimol
mt	Mammillothalamic tract
μm	Micrometer
NBT	Nitroblue tetrazolium
O/N	Overnight
PBS	Phosphate buffered saline
PEI	Polyethylenimine
PMSF	Phenylmethylsulfonyl fluoride
PMBSF	Posteromedial barrel subfield
Po	Posterior nuclear group of the thalamus
P7	Postnatal day 7
(q)PCR	(Quantitative) Polychain reaction
R	Number of scorers
RT	Room temperature
S1	Primary somatosensory
SDS-PAGE	Sodium dodecyl sulfate polyacrylamide gel electrophoresis
SOC	Superior olivary complex
SP	Stratum pyramidale
SPB	Suprapyramidal bundle
Spo	Synaptoporin
V1	Primary visual cortex
WT	Wildtype

Disclosure of potential conflicts of interest

No potential conflicts of interest were disclosed.

Acknowledgments

We thank Jan Sprengers and Roland van Dijk for their contribution to the Nissl staining; Julie Tastet and Eljo van Battum for discussion of the measurements of the hippocampal

parameters. Thanks go to Kim van Elst for her assistance in the behavioral test setup. We thank Asami Oguro-Ando for sharing her knowledge and experience. We are grateful for receiving the Cntn5 mutant animals from Dr. K. Watanabe and the purified Cntn5 peptide for antibody generation from Dr. S. Bouyain.

Funding

This study was supported by Innovative Medicines Initiative Joint Undertaking under Grant Agreement No. 115300 (EU-AIMS), resources of which are composed of financial contribution from the European Union's Seventh Framework Program (FP7/2007–2013) and EFPIA companies' in kind contribution.

References

[1] Burbach JPH, van der Zwaag B. Contact in the genetics of autism and schizophrenia. Trends Neurosci [Internet] 2009; 32:69-72. Available from: http://www.ncbi.nlm.nih.gov/pubmed/19135727; PMID:19135727; https://doi.org/10.1016/j.tins.2008.11.002

[2] van Daalen E, Kemner C, Verbeek NE, van der Zwaag B, Dijkhuizen T, Rump P, Houben R, van't Slot R, de Jonge MV, Staal WG, et al. Social Responsiveness Scale-aided analysis of the clinical impact of copy number variations in autism. Neurogenetics [Internet] 2011 [cited 2012 Aug 6]; 12:315-23. Available from: http://www.pubmedcentral.nih.gov/articlerender.fcgi?artid=3215885&tool=pmcentrez&rendertype=abstract; PMID:21837366; https://doi.org/10.1007/s10048-011-0297-2

[3] Nava N, Chen F, Wegener G, Popoli M, Nyengaard JR. A new efficient method for synaptic vesicle quantification reveals differences between medial prefrontal cortex perforated and nonperforated synapses. J Comp Neurol [Internet] 2014 [cited 2014 Oct 22]; 522:284-97. Available from: http://www.ncbi.nlm.nih.gov/pubmed/24127135; PMID: 24127135; https://doi.org/10.1002/cne.23482

[4] Mercati O, Huguet G, Danckaert A, André-Leroux G, Maruani A, Bellinzoni M, Rolland T, Gouder L, Mathieu A, Buratti J, et al. CNTN6 mutations are risk factors for abnormal auditory sensory perception in autism spectrum disorders. Mol Psychiatry [Internet] 2016; 21:1-9. Available from: http://www.ncbi.nlm.nih.gov/pubmed/27166760; PMID:26678307

[5] Murdoch JD, Gupta AR, Sanders SJ, Walker MF, Keaney J, Fernandez T V, Murtha MT, Anyanwu S, Ober GT, Raubeson MJ, et al. No Evidence for association of autism with rare heterozygous point mutations in contactin-associated protein-like 2 (CNTNAP2), or in other contactin-associated proteins or contactins. PLOS Genet [Internet] 2015; 11:e1004852; PMID:25621974; https://doi.org/10.1371/journal.pgen.1004852

[6] Shimoda Y, Watanabe K. Contactins. Cell Adh Migr 2009; 3:64-70; PMID:19262165; https://doi.org/10.4161/cam.3.1.7764

[7] Zuko A, Kleijer KT, Oguro-Ando A, Kas MJ, van Daalen E, van der Zwaag B, Burbach JP. Contactins in the neurobiology of autism. Eur J Pharmacol [Internet] 2013 [cited 2013 Aug 13]; 719:63-74. Available from: http://www.ncbi.nlm.nih.gov/pubmed/23872404

[8] Lionel AC, Crosbie J, Barbosa N, Goodale T, Thiruvahindrapuram B, Rickaby J, Gazzellone M, Carson AR, Howe JL, Wang Z, et al. Rare copy number variation discovery and cross-disorder comparisons identify risk genes for ADHD. Sci Transl Med 2011; 3:95ra75; https://doi.org/10.1126/scitranslmed.3002464

[9] Nakabayashi K, Komaki G, Tajima A, Ando T, Ishikawa M, Nomoto J, Hata K, Oka A, Inoko H, Sasazuki T, et al. Identification of novel candidate loci for anorexia nervosa at 1q41 and 11q22 in Japanese by a genome-wide association analysis with microsatellite markers. J Hum Genet 2009; 54:531-7; PMID:19680270; https://doi.org/10.1038/jhg.2009.74

[10] Nikpay M, Šeda O, Tremblay J, Petrovich M, Gaudet D, Kotchen T a, Cowley AW, Hamet P. Genetic mapping of habitual substance use, obesity-related traits, responses to mental and physical stress, and heart rate and blood pressure measurements reveals shared genes that are overrepresented in the neural synapse. Hypertens Res [Internet] 2012 [cited 2012 Aug 6]; 35:585-91. Available from: http://www.pubmedcentral.nih.gov/articlerender.fcgi?artid=3368234&tool=pmcentrez&rendertype=abstract; PMID:22297481; https://doi.org/10.1038/hr.2011.233

[11] Harold D, Abraham R, Hollingworth P, Sims R, Gerrish A, Hamshere ML, Pahwa JS, Moskvina V, Dowzell K, Williams A, et al. Genome-wide association study identifies variants at CLU and PICALM associated with Alzheimer' s disease. Nat Genet 2009; 41:1088-93.

[12] Lambert J, Heath S, Even G, Campion D, Sleegers K, Hiltunen M, Combarros O, Zelenika D, Bullido MJ, Tavernier B, et al. Genome-wide association study identifies variants at CLU and CR1 associated with Alzheimer ' s disease. Nat Genet [Internet] 2009; 41:1094-9; PMID:19734903; https://doi.org/10.1038/ng.439

[13] Li H, Takeda Y, Niki H, Ogawa J, Kobayashi S, Kai N, Akasaka K, Asano M, Sudo K, Iwakura Y, et al. Aberrant responses to acoustic stimuli in mice deficient for neural recognition molecule NB-2. Eur J Neurosci [Internet] 2003 [cited 2012 Jul 30]; 17:929-36; PMID:12653969; https://doi.org/10.1046/j.1460-9568.2003.02514.x

[14] Toyoshima M, Sakurai K, Shimazaki K, Takeda Y, Shimoda Y, Watanabe K. Deficiency of neural recognition molecule NB-2 affects the development of glutamatergic auditory pathways from the ventral cochlear nucleus to the superior olivary complex in mouse. Dev Biol [Internet] 2009 [cited 2013 Feb 1]; 336:192-200. Available from: http://www.ncbi.nlm.nih.gov/pubmed/19818338; PMID:19818338; https://doi.org/10.1016/j.ydbio.2009.09.043

[15] Toyoshima M, Sakurai K, Shimazaki K, Takeda Y, Nakamoto M, Serizawa S, Shimoda Y, Watanabe K. Preferential localization of neural cell recognition molecule NB-2 in developing glutamatergic neurons in the rat auditory brainstem. J Comp Neurol [Internet] 2009 [cited 2012 Jul 30]; 513:349-62. Available from: http://www.ncbi.nlm.nih.gov/pubmed/19177518; PMID:19177518; https://doi.org/10.1002/cne.21972

[16] Zuko A, Oguro-Ando A, van Dijk R, Gregorio-Jordan S, van der Zwaag B, Burbach JPH. Developmental role of the cell adhesion molecule Contactin-6 in the cerebral cortex and hippocampus. Cell Adh Migr 2016; 10:378-92.

[17] Molenhuis RT, Visser L De, Bruining H, Kas MJ. Enhancing the value of psychiatric mouse models; differential expression of developmental behavioral and cognitive pro fi les in four inbred strains of mice. Eur Neuropsychopharmacol [Internet] 2014; 24:945-54; PMID:24491952; https://doi.org/10.1016/j.euroneuro.2014.01.013

[18] Kleijer KTE, Zuko A, Shimoda Y, Watanabe K, Burbach JPH. Contactin-5 expression during development and wiring of the thalamocortical system. Neuroscience 2015; 310:106-13; PMID:26391921

[19] Puelles L, Martinez-de-la-Torre M, Bardet S, Rubenstein JLR. The Mouse Nervous System. 1st ed. Elsevier; 2012.

[20] Tasic B, Menon V, Nguyen TNT, Kim TTK, Jarsky T, Yao Z, Levi BB, Gray LT, Sorensen SA, Dolbeare T, et al. Adult mouse cortical cell taxonomy revealed by single cell transcriptomics. Nat Neurosci [Internet] 2016; advance on 19:335-46. Available from: https://doi.org/10.1038/nn.4216

[21] Heyden A, Angenstein F, Sallaz M, Seidenbecher C, Montag D. Abnormal axonal guidance and brain anatomy in mouse mutants for the cell recognition molecules close homolog of L1 and NgCAM-related cell adhesion molecule. Neuroscience 2008; 155:221-33; PMID:18588951; https://doi.org/10.1016/j.neuroscience.2008.04.080

[22] Montag-Sallaz M, Schachner M, Montag D. Misguided axonal projections, neural cell adhesion molecule 180 mRNA upregulation, and altered behavior in mice deficient for the close homolog of L1 misguided axonal projections, neural cell adhesion molecule 180 mRNA upregulation, and altered behavi. Mol Cell Biol 2002; 22:7967-81.

[23] Ogawa J, Kaneko H, Masuda T, Nagata S, Hosoya H, Watanabe K. Novel neural adhesion molecules in the Contactin/F3 subgroup of the immunoglobulin superfamily: isolation and characterization of cDNAs from rat brain. Neurosci Lett 1996; 218:173-6; PMID:8945756; https://doi.org/10.1016/S0304-3940(96)13156-6

[24] Yoshihara Y, Kawasaki M, Tamada A, Nagata S, Kagamiyama H, Mori K. Overlapping and differential expression of BIG-2, BIG-I TAG-I and F3: four members of an axon-associated cell adhesion molecule subgroup of the immunoglobulin superfamily. J Neurobiol 1995; 28:51-69; PMID:8586965; https://doi.org/10.1002/neu.480280106

[25] Diamond ME, Armstrong-James M, Budway MJ, Ebner FF. Somatic sensory responses in the rostral sector of the posterior group (POm) and in the ventral posterior medial nucleus (VPM) of the thalamus: Dependence on the barrel field cortex. J Comp Neurol 1992; 319:66-84; PMID:1592906; https://doi.org/10.1002/cne.903190108

[26] Cremer H, Chazal G, Goridis C, Represa A. NCAM is essential for axonal growth and fasciculation in the hippocampus. Mol Cell Neurosci 1997; 8:323-35; PMID:9073395; https://doi.org/10.1006/mcne.1996.0588

[27] Pierce K, Courchesne E. Evidence for a cerebellar role in reduced exploration and stereotyped behavior in autism. Biol Psychiatry 2001; 49:655-64; PMID:11313033; https://doi.org/10.1016/S0006-3223(00)01008-8

[28] Koterba EA, Leezenbaum NB, Iverson JM. Object exploration at 6 and 9 months in infants with and without risk for autism. Autism [Internet] 2014; 18:97-105. Available from: http://www.pubmedcentral.nih.gov/articlerender.fcgi?artid=3773524&tool=pmcentrez&rendertype=abstract; PMID:23175749; https://doi.org/10.1177/1362361312464826

[29] Pearson BL, Pobbe RLH, Defensor EB, Oasay L, Bolivar VJ, Blanchard DC, Blanchard RJ. Motor and cognitive stereotypies in the BTBR T+tf/J mouse model of autism. Genes, Brain Behav 2011; 10:228-35; https://doi.org/10.1111/j.1601-183X.2010.00659.x

[30] Kas MJ, Glennon JC, Buitelaar J, Ey E, Biemans B, Crawley J, Ring RH, Lajonchere C, Esclassan F, Talpos J, et al. Assessing behavioural and cognitive domains of autism spectrum disorders in rodents: current status and future perspectives. Psychopharmacology (Berl) [Internet] 2013 [cited 2013 Oct 31]; 231:1125-46 Available from: http://www.ncbi.nlm.nih.gov/pubmed/24048469; PMID:24048469

[31] Antunes M, Biala G. The novel object recognition memory: neurobiology, test procedure, and its modifications. Cogn Process 2012; 13:93-110.

[32] Dudova I, Vodicka J, Havlovicova M, Sedlacek Z, Urbanek T, Hrdlicka M. Odor detection threshold, but not odor identification, is impaired in children with autism. Eur Child Adolesc Psychiatry 2011; 20:333-40; PMID:21528391; https://doi.org/10.1007/s00787-011-0177-1

[33] Molenhuis RT, Bruining H, Remmelink E, de Visser L, Loos M, Burbach JPH, Kas MJH. Limited impact of Cntn4 mutation on autism-related traits in developing and adult C57BL/6J mice. J Neurodev Disord [Internet] 2016; 8:6. Available from: http://www.pubmedcentral.nih.gov/articlerender.fcgi?artid=4782374&tool=pmcentrez&rendertype=abstract; PMID:26958094; https://doi.org/10.1186/s11689-016-9140-2